Development of practical method of determining rock anisotropy using a large hollow cylinder

Koichi Shin (Central Research Institute of Electric Power Industry, Japan)

1. Introduction

1.1 Examples of anisotropy in rocks

Rocks have anisotropy in the scale from a centimeter for rock matrix, to a few tens of meter for construction scale, to a geological rock mass scale, and to the crustal scale. And it is not so rare that the anisotropy ratio is so large as more than 2. Anisotropy comes from the structure of rock and is exhibited in strength, deformability, elastic wave velocity, permeability, etc.

In the scale of laboratory specimen, mineral arrangement in sedimentary rocks and microcrack alignment in crystalline rocks can sometimes cause anisotropy ratio of more than 2 in elasticity[1)].

In the scale of construction such as tunnel or cavern, layered rocks and/or rock with concentrated joint distribution can have large anisotropy. For example, plate jack tests at a layered rock site in Japan showed 1.5 times larger Young's modulus in the direction parallel to the bedding plane than in the direction normal to it[2)]. For a dam site in Portugal, anisotropy ratio of about 3 in elasticity is reported[3)].

In the scale of the crust, its anisotropy has been detected through seismic wave analysis all over the world including the Antarctic. It has been observed mainly through the polarization of S wave. The velocity difference of S_v and S_h are reported to be 2% to 10%. The mantle below the crust is also reported[4)] to have anisotropy to the depth of at least 300km. A measurement at Hyogo, Japan has shown 11% polarization of S wave[5)] in the depth range of 6 to 8 km.

1.2 Necessity of anisotropy evaluation

It has been pointed out for example in the field of theory of elasticity that assuming isotropy for an anisotropic material can cause large error[6)7)]. For this reason, the importance of anisotropy in geo-engineering issues has been stressed[8)] so far, but in practical engineering anisotropy determination in the scale of in-situ rock test is rare. One of the reasons for this might be that there is no practical method, because of too many anisotropy parameters and because of variation of properties in space. And maybe because in the past 3 dimensional evaluation of anisotropy was not needed, simple 2D evaluation was good enough for 2D analysis of tunnel or cavern. But in this age of computer evolution, 3D analysis is beginning to be required for more rational design. For the 3D analysis, 3D anisotropy is needed to be determined.

One of the urgent issues of this modern world depending on nuclear energy is the construction of underground disposal facility of nuclear waste. To this underground facility, not only the function of keeping the cavern space but also the barrier function against radioactive nuclide transportation for very long time duration are required. Therefore, rock characterization and rock evaluation should be more rigorous than for conventional underground construction. Especially the near-field rock around the deposition hole which contains HLW canister with bentonite buffer needs to be investigated in detail because the near-field rock and bentonite interact with each other and can have some effects on barrier function against the nuclide transportation. If anisotropy exists, it should be evaluated in detail.

1.3 The targets of the development

Anisotropy can exist in different scales as stated in 1.1. When we are to evaluate the near-field rock

around the HLW deposition hole, the scale of the test should be similar to the scale of the deposition hole. The centimeter scale for laboratory test would be too small and ten meter scale for cross hole seismic testing would be too large. The scale of plate jack testing for example would be good for the evaluation of rock around the deposition hole.

As we experience in in-situ rock tests such as rock shear test and plate jack test, even within a same geological and geo-technical categorization, rock properties can change considerably from place to place. Since there are more than a few parameters to be determined for anisotropy, some plural tests may usually be required to determine a set of anisotropy. In such a case the variation of properties from place to place can hinder and distort the anisotropy determination. It would very much be preferred to have a method which requires one specimen to determine a set of anisotropy.

Another point of consideration would be that the method be whether seismic test or loading test. Since the anisotropy around the deposition hole would mainly be taken into account in the evaluation of mechanical interaction with bentonite under the in-situ stress condition, the loading test would be much better. And to avoid uneven and/or eccentric loading, pressurization using a jacket would be preferable than loading via platen.

And at last, the method wants to be able to treat 3 dimensional orthogonal anisotropy, which would be good enough for geo-engineering, rather than only layered body or transverse isotropy. Further, the method wants to be valid even if the directions of anisotropy axes are unknown.

This paper describes the methodology of the developed method of determining anisotropy which can meet the above-mentioned targets.

2. Plan of the development

2.1 Mode of testing

In principle, there can be various types of testing for determining anisotropy, such as seismic velocity tests using cores in directions more than a few[9], axial loading tests using cores in plural directions, in-situ plate jack tests in plural directions, etc. Oka and Hirashima[10] have made a theoretical study to determine 2D orthogonal anisotropy by plate jack test and by tunnel pressure test.

In this paper, as shown in 1.3 as the targets of the development, a method which uses a relatively large rock sample and can determine a set of anisotropy using a single specimen by pressurization test is considered. For this purpose hollow cylinder is considered. The concept of the mode of testing is shown in Fig.1. The response of displacement measured in the center hole of the cylinder when its outer surface is pressurized will be used for the anisotropy determination. Both ends of the cylinder will be capped and the entire cylinder be jacketed for the pressurization.

The principle of setting pressure level will follow that of in-situ tests such as plate jack test. The pressure level will be roughly similar to the in-situ stress level because we want to know the rock deformation characteristics at such stress level. About the size of the cylinder, diameter 20 cm and length about 1 m would be easily possible because such cylinder has been already used many times for overcoring stress measurement in Japan.

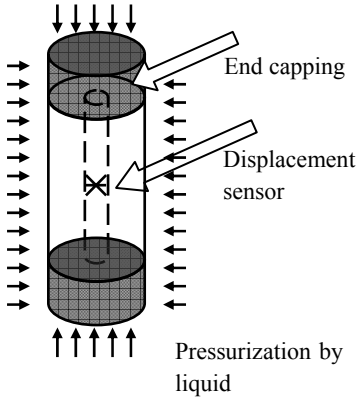

Fig.1 Concept of testing

2.2 Procedure of the development

To determine anisotropy from the deformation response to pressurization, one of probable procedures would consist of the following.

(1) Realizing forward analysis of determining the deformation of the center hole of the anisotropic cylinder subjected to pressurization,

(2) Reducing the number of independent parameters of anisotropy with little sacrifices, if possible. This is important because one of the reasons that anisotropy is not usually measured in practical geo-engineering is that determining parameters of more than a few is too difficult. If the number of parameters can be reasonably reduced, it means a lot.

(3) Formulating back analysis to determine anisotropy from the measured deformation of the inner hole, and also confirming stability of the back analysis. Generally speaking, back analysis does not always give correct answer but can give some false answers. Stability of a back analysis is necessary to obtain a correct anisotropy.

In the following sections, above-mentioned 3 items are discussed.

3. Solution of center hole deformation of an anisotropic cylinder

3.1 Policy to obtain the solution

Setting aside folding, anisotropy of rocks is on orthogonal coordinates. The present problem is to find a solution of center hole deformation of a hollow cylinder sampled out in arbitrary direction from such anisotropic rock. Since theoretical solution was not found in literature, the author has tried to make a simple solution which is good enough for present purpose. FEM is good only for forward analysis but it does not suffice for backward analysis because backward analysis requires huge numbers of iterating forward analysis and therefore FEM is not practical for present purpose.

Fig.2 is the flowchart of steps to obtain a simple solution. First, many anisotropy cases are generated including the consideration of directions of anisotropy, and the center hole deformation of a hollow cylinder is determined by 3D FEM analysis. Second, hole deformation of an infinite body of the same anisotropy is determined using Amadei's theoretical solution[6]. Then thirdly, the deformation of the hollow cylinder is expressed as the product of coefficient and deformation of a hole in the infinite body. Then fourthly, the coefficient is evaluated as a function of anisotropy parameters.

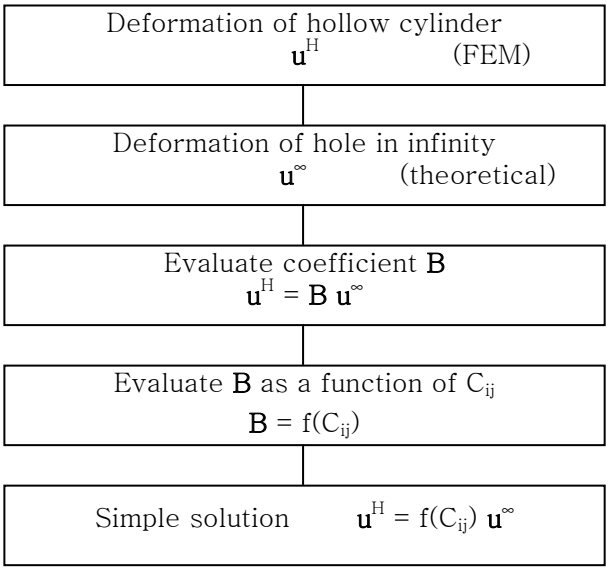

Fig.2 Steps to obtain simple solution of center hole deformation of a hollow cylinder

3.2 FEM analysis

3.2.1 FEM model and discretization error

The ratio between center hole diameter and outer diameter is set to be 1/4. This ratio is adopted for an overcoring method for stress measurement in Japan. The FEM code ABAQUS has been used. 3D model of a hollow cylinder with the height 2.5 times the outer diameter has been established and the deformation has been evaluated at the central height. A quarter region of the transverse section is shown in Fig.3. The size of element in radial direction has been determined considering the stress distribution around the hole. The total number of elements is 144,000. The difference between the deformation in this FEM model and theoretical deformation in the case of isotropy is less than 0.02%. The discretization error in this FEM model is thought to be negligible.

3.2.2 Anisotropy cases

The number of anisotropy is 17 disregarding the coordinate transformation. The parameters of each case are shown in Table 1. In the table, C_{ij} is an element of elasticity matrix. By coordinate transformation, 588(=7*7*12) cases for each basic anisotropy, and 9996(=588*17) cases in total have been generated. The increment of transformation rotation angle is 30 degrees for x and y and 15 for z.

The parameters in Table 1 have been determined as follows. When an isotropic elastic medium contains penny shaped micro cracks, the resultant bulk elasticity can be theoretically calculated by Hudson's formulation[11]. Density, type whether hollow or shear of micro cracks in 3 orthogonal directions, and poisson's ratio of the matrix have been changed to obtain the 17 basic anisotropies shown in Table 1. Density of micro crack is $N c_r^3/V$ where N is the number of micro crack in the volume V and c_r is the radius of the penny shaped micro crack. Between the both surfaces of a micro crack, there is no force for hollow type and only normal force for shear type.

As shown in Table 1, the maximum ratio of anisotropy is 2.08 for normal elasticity and 2.18 for shear elasticity.

As a more general anisotropy than orthogonal, triclinic anisotropy is generated for the later verification of the solution we are going to obtain, together with two cases of transverse isotropy.

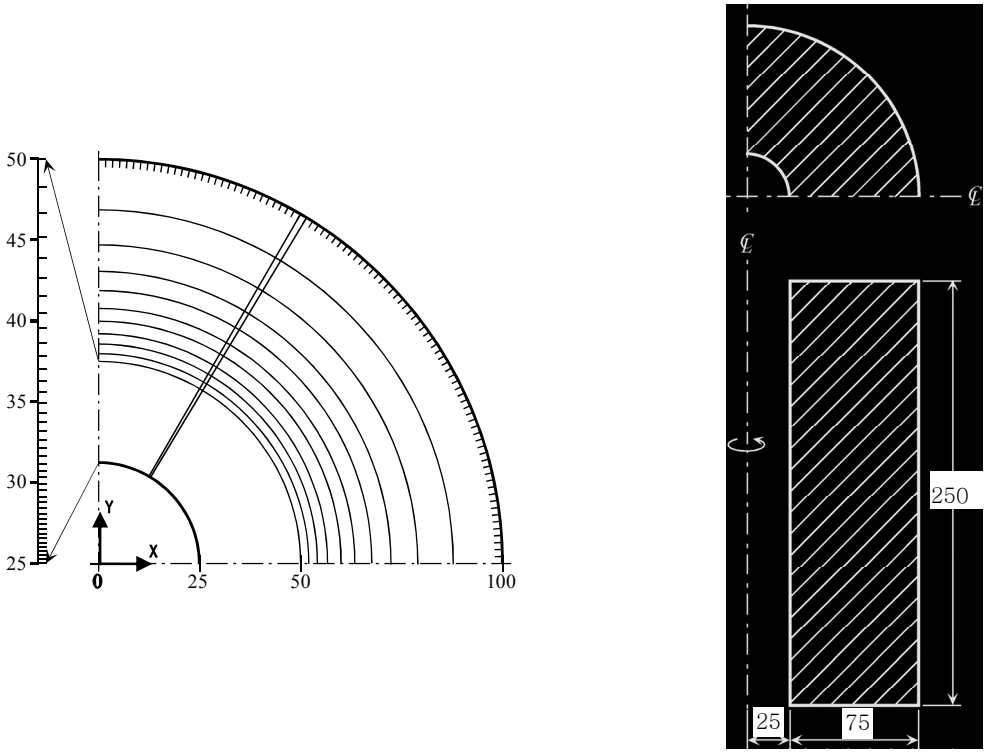

Fig.3 FEM mesh model

Table 1. Elastic parameters for anisotropic cases

(17 orthogonal, 2 transverse isotropy and 1 triclinic cases)

	C_{11}	C_{22}	C_{33}	C_{44}	C_{55}	C_{66}	C_{23}	C_{31}	C_{12}	normal ratio	shear ratio
OR 1	1.201	0.985	0.770	0.233	0.283	0.334	0.238	0.302	0.367	1.559	1.436
OR 2	1.346	1.346	1.346	0.233	0.283	0.334	0.577	0.577	0.577	1.000	1.436
OR 3	1.136	0.777	0.562	0.165	0.249	0.300	0.087	0.195	0.259	2.022	1.819
OR 4	1.346	1.346	1.346	0.165	0.249	0.300	0.577	0.577	0.577	1.000	1.819
OR 5	1.322	1.286	1.250	0.359	0.368	0.376	0.520	0.531	0.542	1.057	1.047
OR 6	1.346	1.346	1.346	0.359	0.368	0.376	0.577	0.577	0.577	1.000	1.047
OR 7	1.017	0.853	0.689	0.248	0.317	0.386	0.058	0.075	0.091	1.475	1.556
OR 8	1.023	1.023	1.023	0.248	0.317	0.386	0.114	0.114	0.114	1.000	1.556
OR 9	1.014	0.741	0.578	0.156	0.271	0.340	0.034	0.061	0.078	1.756	2.178
OR 10	1.023	1.023	1.023	0.156	0.271	0.340	0.114	0.114	0.114	1.000	2.178
OR 11	1.022	0.994	0.967	0.420	0.432	0.443	0.104	0.107	0.110	1.056	1.055
OR 12	1.023	1.023	1.023	0.420	0.432	0.443	0.114	0.114	0.114	1.000	1.055
OR 13	1.320	0.977	0.634	0.229	0.271	0.314	0.194	0.331	0.469	2.081	1.375
OR 14	2.143	2.143	2.143	0.229	0.271	0.314	1.429	1.429	1.429	1.000	1.375
OR 15	2.143	2.143	2.143	0.171	0.243	0.286	1.429	1.429	1.429	1.000	1.667
OR 16	2.006	1.949	1.891	0.336	0.343	0.350	1.223	1.246	1.269	1.060	1.043
OR 17	2.143	2.143	2.143	0.336	0.343	0.350	1.429	1.429	1.429	1.000	1.043
TV 1	1.217	1.217	0.643	0.249	0.249	0.385	0.275	0.275	0.448	1.894	1.542
TV 2	1.510	1.510	1.179	0.303	0.303	0.509	0.465	0.465	0.491	1.280	1.681

TR $[C_{ij}]$ =

1.201	0.367	0.302	-0.065	0.000	0.000
0.367	0.927	0.296	-0.108	0.000	0.000
0.302	0.296	0.712	-0.108	0.000	0.000
-0.065	-0.108	-0.108	0.291	0.000	0.000
0.000	0.000	0.000	0.000	0.283	-0.051
0.000	0.000	0.000	0.000	-0.051	0.334

3.2.3 External pressurization and evaluation of deformation

In the FEM analysis, unit pressure has been applied only on the lateral surface of the cylinder. The deformation for the axial loading can simply be obtained without executing FEM analysis. In this way, we will be able to handle the lateral surface pressurization and axial pressurization independently when necessary.

Fig.4 shows an example of deformation of a hollow cylinder subjected to pressurization on the lateral surface. The both ends are parallelly undulating.

Based on the FEM analysis, the displacement in r direction at the point (r_a, 0, 0) is normalized by the radius r_a and expressed as u_r^H. Also the displacement in z direction at the same point is normalized and expressed as u_z^H. Further, strain in z direction ε_z^H at the same point is evaluated. The solutions for other points which are the rotation around z axis is obtained from the solution at (r_a, 0, 0) for other anisotropies obtained by rotation of the anisotropy around z axis. In this way the deformation of the center hole is

expressed by u_r^H, u_z^H and ε_z^H . Using these three parameters, the displacement between any 2 points on the surface of center hole can be obtained when the 2 point is point symmetric regarding a point on the axis of the cylinder.

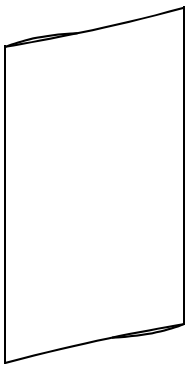

Fig.4 An example of deformation of a hollow cylinder subjected to pressurization on the outer lateral surface. (Dash line shows the shape before pressurization.)

3.3 Finding a function of the solution by regression

The ratio between the normalized displacements u_r^H and u_z^H and strain ε_z^H at the point (r_a, 0, 0) for the hollow cylinder and those for the hole in infinite body, for each of 9996 cases of orthogonal anisotropy, have been calculated to be denoted as B_r, B_z and B_{ez}. The far field stress for the hole in infinite body is set as $\sigma_x = \sigma_y = 1$, $\sigma_z = \tau_{xy} = \tau_{yz} = \tau_{zx} = 0$ corresponding to the unit pressurization on the outer lateral pressurization on the hollow cylinder. The normalized displacements u_r^∞ and u_z^∞ and strain ε_z^∞ at the point (r_a, 0, 0) for the hole in infinite body can be obtained according to Amadei[6].

$$u_r^H = B_r\, u_r^\infty$$
$$u_z^H = B_z\, u_z^\infty$$
$$\varepsilon_z^H = B_{ez}\, \varepsilon_z^\infty \qquad (1)$$

The coefficients B_r, B_z and B_{ez} are functions only of anisotropic elastic parameters C_{ij}, because the ratio between the internal and outer diameters is fixed to 1/4 as stated in section 3.2.

$$B_r = fn_r(C_{ij})$$
$$B_z = fn_z(C_{ij})$$
$$B_{ez} = fn_{ez}(C_{ij}) \qquad (2)$$

Several model functions were set for each of B_r, B_z and B_{ez} and the result of regression analysis were compared. As a result, the following functions have been found to be the best.

$$B_r = \sum_{l=1}^{6}\sum_{k=1}^{6}\sum_{j=1}^{6}\sum_{i=1}^{6}[b^r_{ijkl}\ a_{ij}\ a_{kl}]/a_{33}^2$$
$$B_z = \sum_{l=1}^{6}\sum_{k=1}^{6}\sum_{j=1}^{6}\sum_{i=1}^{6}[b^z_{ijkl}\ a_{ij}\ a_{kl}]/a_{33}^2 \qquad (3)$$
$$B_{ez} = \sum_{l=1}^{6}\sum_{k=1}^{6}\sum_{j=1}^{6}\sum_{i=1}^{6}[b^{ez}_{ijkl}\ a_{ij}\ a_{kl}]/a_{33}^2$$

$i \le j$, $k \le l$, $i \le k$.
when $i = k$, $j \le l$.

a_{ij} is the element of compliance matrix which is the inverse of elasticity matrix $[C_{ij}]$. And b^r_{ijkl}, b^z_{ijkl}

and b^{ez}_{ijkl} are coefficients determined by regression analysis, with 231 elements respectively. These regression functions have maximum error of 0.8% of u_r^H for all anisotropy cases of 9996, and thus these functions in (1) are good solution of deformation of the center hole of the anisotropic hollow cylinder.

3.4 Verification of the solution

To verify the solution obtained in section 3.3, three basic anisotropies which have not been used in the regression analysis to determine the solution, have been set as shown in Table 1. Two are transverse isotropy and one is triclinic anisotropy. Triclinic anisotropy is the most general anisotropy with 21 independent parameters and three anisotropic axes are not orthogonal to each other any more. One of the two transverse isotropy has been established based on Hudson's elasticity model[11] with a micro crack system aligned at one direction. Another one has been established as a layered medium based on Salamon[12] (Table 2). Φ_j in the table is the ratio of the j^{th} layer's thickness. E, ν and G are the elastic parameters in the isotropic plane and E', ν' and G' are the parameters outside of the isotropic plane.

Table 2. Macroscopic parameters of transverse isotropy for layer structure of different isotropic media. (Salamon, 1968)[12]

$$
\begin{aligned}
1/E &= \sum_j [\Phi_j E_j/(1-\nu^2{}_j)] \;/\; [\{\sum_j \Phi_j E_j/(1+\nu_j)\}\ \{\sum_j \Phi_j E_j/(1-\nu_j)\}] \\
1/E' &= \sum_j \Phi_j \{1/E' - 2\nu'^2{}_j E_j/(E_j'(1-\nu_j)) + 2\{\sum_j \Phi_j E_j \nu_j'/E_j'/(1-\nu_j)\}^2 \\
&\quad /\{\sum_j \Phi_j E_j/(1-\nu_j)\} \\
\nu/E &= \sum_j \{\Phi_j E_j \nu_j/(1-\nu^2{}_j)\}\ /[\{\sum_j \Phi_j E_j/(1+\nu_j)\}\ \{\sum_j \Phi_j E_j/(1-\nu_j)\}] \\
\nu'/E' &= \sum_j \{\Phi_j E_j \nu_j'/E'(1-\nu_j)\}/\ \{\sum_j \Phi_j E_j/(1-\nu_j)\} \\
1/G &= 1/\sum_j \Phi_j G_j \quad , \quad 1/G' = \sum_j \Phi_j/G_j'
\end{aligned}
$$

For the anisotropy cases of 1764 (7*7*12 *3) obtained by the rotation transformation of the three basic anisotropies, the hole deformation u_r^H, u_z^H and strain ε_z^H obtained from the solution, eq.(1), and those from FEM analysis have been compared. An example of graphical comparison is shown in Fig.5, for u_r^H in the case of triclinic anisotropy. The vertical axis is for the normalized displacement u_r^H. The horizontal axis is for 588 cases generated by rotation transformation of the triclinic. The plots are for the simple solution of eq.(1), and the line is for the FEM results. Not only u_r^H but also u_z^H and ε_z^H have been found to be agreeing with the FEM results. Also, this agreement has been found in the two cases of transverse isotropy. Thus eq.(1) has been found to be a good enough solution of center hole deformation of a hollow cylinder of general anisotropy. Note that the error in the deformation of isotropic thick hollow cylinder has been 0.6% between the theoretical solution and eq.(1).

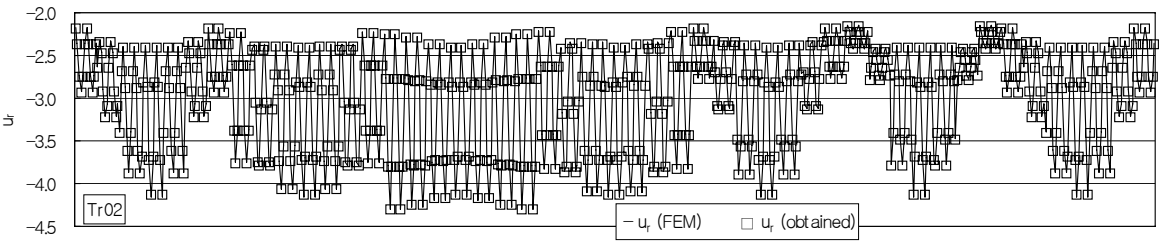

Fig.5 An example of comparison between deformation by FEM and the simple solution.
Horizontal axis is for 588 cases of rotation-transformed triclinic anisotropy.
(solid line for FEM, square dots for the simple solution)

3.5 Conclusion about the solution

From the results of regression analysis in section 3.3 and verification in 3.4, the obtained simple solution eq.(1) of the center hole deformation of a hollow cylinder has been found to be accurate enough for transverse isotropy, orthogonal anisotropy and triclinic anisotropy with maximum stiffness ratio of up to about 2. This solution is simple and easy to use for back analysis which will require huge number of iterative calculations.

4. Reducing the number of independent parameters of orthogonal anisotropy

4.1 Policy to reduce the number

When we adopt anisotropy instead of isotropy for the purpose of describing the behaviour of geo-material, we then meet the obstacle of many parameters. The very simple anisotropy of transverse isotropy for example have 5 independent parameters. More practical anisotropy of orthogonal have 9 independent parameters. When the directions of anisotropic axes are unknown, 3 additional independent parameters have to be determined.

The difficulty and complication arising from the above-mentioned problem is one of the reasons that in practical geo-engineering the evaluation of anisotropy has been prone to be avoided. And even when anisotropy is to be evaluated, some restrictions may be required, for example, transverse isotropy may be adopted for a rock with clear evidence of orthogonal anisotropy as a compromise.

In this chapter, a mean to describe orthogonal anisotropy as accurate as possible with a number of independent parameters as less as possible is sought. .

The number of independent parameters 5 for transverse isotropy and 9 for orthogonal anisotropy for example are deduced from mathematical consideration of symmetry. Geo-materials such as soil and rock are composite of mineral particles, layered body and/or micro cracked body. Therefore there may exist a further restrictions coming from the micro-structural features on the anisotropic parameters.

Therefore, possible relationships between independent anisotropic parameters have been studied for layered body and micro-cracked body through numerical calculation. The anisotropy cases used for this study are shown in Table 3. If we find some relationships, then we can reduce the number of independent parameters based on them. The relationships will be verified by the previous measurements of anisotropy of soil and rock.

Table 3. Cases of anisotropic bodies used for consideration of reducing number of independent parameters.

Case (1):	repetition of 2 kinds of layers
Case (2):	repetition of 3 kinds of layers
Case (3):	penny cracks in one direction
Case (4):	penny cracks normal randomly aligned in a plane
Case (5):	penny cracks normal randomly aligned with an angle from the plane
Case (6):	penny cracks aligned in 3 orthogonal directions
Case (7):	combination of Case 3 and Case 5

Orthogonal anisotropy is considered for the present purpose. 9 independent parameters C_{11}, C_{22}, C_{33}, C_{44}, C_{55}, C_{66}, C_{12}, C_{23} and C_{31} are rearranged using new parameters k_{g1}, k_{g2}, k_{g3}, k_{v12}, k_{v23} and k_{v13} as follows.

$k_{g1} \equiv C_{44}/(C_{22}+C_{33})$, $k_{g2} \equiv C_{55}/(C_{33}+C_{11})$
$k_{g3} \equiv C_{66}/(C_{11}+C_{22})$
$k_{v12} \equiv C_{12}/(C_{11}+C_{22})$, $k_{v13} \equiv C_{13}/(C_{11}+C_{33})$
$k_{v23} \equiv C_{23}/(C_{22}+C_{33})$ (4)

Further, k_{gm} and k_{vm} are introduced.
$k_{gm} \equiv (k_{g1}+ k_{g2}+ k_{g3})/3$
$k_{vm} \equiv (k_{v12}+ k_{v23}+ k_{v13})/3$ (5)

4.2 Anisotropy for micro-cracked body

As stated in section 3.2.2, macroscopic anisotropy of micro-cracked body can be determined according to Hudson[11]. The cases generated are shown as (3), (4), (5), (6) and (7) in Table 3. (3) is the case of aligned micro-cracks only in one direction, (4) is for micro-cracks aligned randomly in a plane, (5) is similar to (4) but the normal of each micro-crack is out of the plane at an angle, (6) is for three micro-crack systems aligned orthogonally, and (7) is a combination of (3) and (5).

Table 4 shows, as an example, parameters for orthogonal case (6), namely, crack density, crack type (hollow or shear), poisson's ratio of matrix. Among all individual anisotropies in case (6), the maximum of anisotropic ratio for normal elasticity has been 1.5 and 1.4 for shear elasticity. Fig.6 shows relationships among k_{g1}, k_{g2}, k_{g3}, k_{v12}, k_{v23}, k_{v13}, k_{gm} and k_{vm}. The following rough relationships are observed in the figure.

$k_{g1} \approx k_{g2} \approx k_{g3} \approx k_{gm}$
$k_{v12} \approx k_{v23} \approx k_{v13} \approx k_{vm}$
$k_{vm} \approx 1/2 - 2\, k_{gm}$ (6)

These relationships have been found also in all other cases of micro-cracked body (3) to (7) in Table 3.

Table 4. Parameters to constitute orthogonal micro crack system (case 6).

	Crack density	Crack type	poisson ration
1st crack system	0, 0.001, 0.01, 0.04	Empty crack Shear crack	0.1, 0.2, 0.3, 0.4
2nd crack system	0, 0.001, 0.01, 0.04		
3rd crack system	0, 0.001, 0.01, 0.04		

maximum ratio of anisotropy for normal elasticity	1.48
maximum ratio of anisotropy for shear elasticity	1.34

4.3 Anisotropy for layered body

Macroscopic anisotropy of layered medium are obtained according to Salamon[12] as stated in section 3.4. Cases (1) and (2) in Table 3 are for the layered bodies, namely repetition of bedding of two kinds of layers and three kinds of layers respectively. Table 5 shows as an example Young's modulus, poisson's ratio, thickness ratio of each layer for case (1). Among all the anisotropies for the case (1), the maximum of anisotropic ratio for normal elasticity has been 1.8 and 1.9 for shear. Fig.7 shows the relationships among the parameters k_{g1} to k_{vm}. From the figure, the rough relationships observed in the micro-cracked body as eq.(6) have also been found to be valid for the layered body. These relationships have also been found for the case (2) in Table 3.

4.4 Measured anisotropy of rocks and sands.

The anisotropy of some rocks and sands has been measured based on elastic wave or loading tests. In

these tests, most cases have been assumed to be transversely isotropy and a few to be orthogonal. Fig.8 shows the relationships among the parameters k_{g1} to k_{vm}. The samples and references are also listed in Table 6. As shown in the figure, the rough relationships of eq.(6) observed theoretically for layered and micro-cracked body are verified by the actual data.

4.5 Conclusion about reducing the number of parameters

A method has been devised to reduce the number of independent parameters of orthogonal anisotropy with minimal sacrifices. First, since the cause of anisotropy of rocks are considered to be structural reason such as layer and/or cracks and joints, theoretical calculations of macroscopic anisotropy have been done for layered and micro-cracked bodies. As the result, it has been found that these structural features pose some restrictions on the 9 independent parameters of orthogonal anisotropy. Eqs.(6) are the rough relationships or restrictions on the parameters. The relationships have been verified by actual data from previous papers. As a result, the following 4 parameters are deduced to be good enough for practical geo-engineering. Namely, C_{11}, C_{22}, C_{33} and k_{gm}.

When we are to characterize a rock to be orthogonal for engineering purpose, only 4 independent parameters will be needed and the elasticity matrix is expressed as in Table 7. k_g and k_v in the table are defined as follows.

$$k_g \equiv (k_{g1} + k_{g2} + k_{g3})/3$$
$$k_v \equiv 1/2 - 2\,k_g \qquad (7)$$

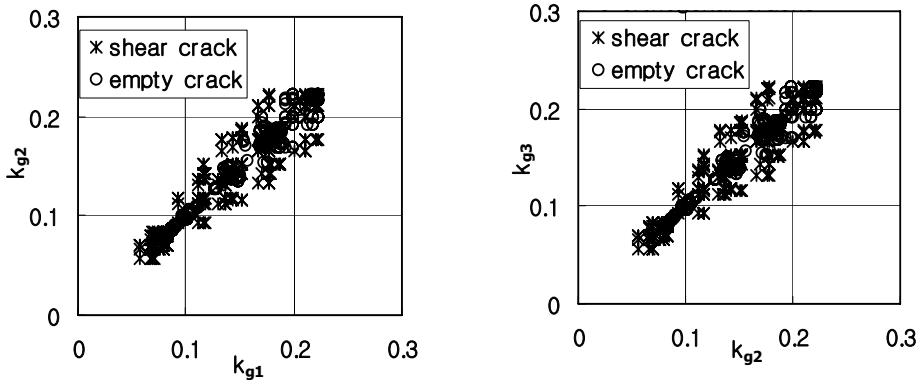

(a) k_{g1} vs k_{g2}

(b) k_{g2} vs k_{g3}

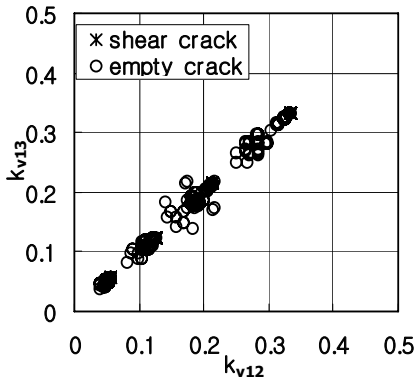

(c) k_{v12} vs k_{v13}

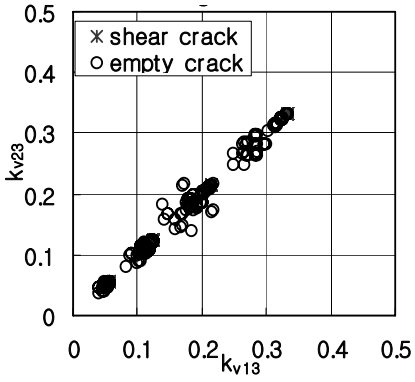

(d) k_{v13} vs k_{v23}

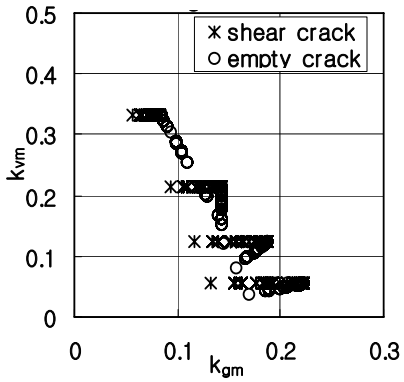

(e) k_{gm} vs k_{vm}

Fig.6 Relationships among elastic parameters.

(case 6. Orthogonal micro crack system)

Table 5. Parameters to constitute 2-layer body (case 1).

	Ei	vi	thickness ratio
1st layer	10	0.1, 0.275, 0.45	0.2, 0.5, 0.8
2nd layer	10,20,40	0.1, 0.275, 0.45	(0.8, 0.5, 0.2)

maximum ratio of anisotropy for normal elastic 1.79

maximum ratio of anisotropy for shear elasticity 1.87

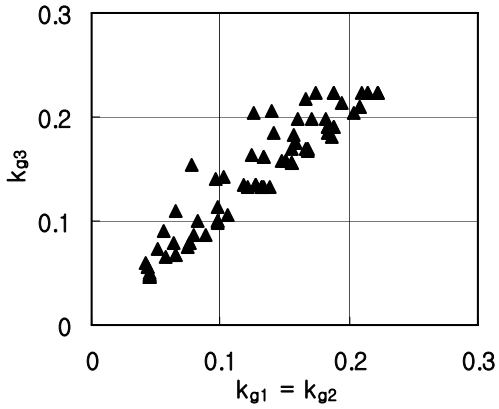

(a) k_{g1} vs k_{g3}

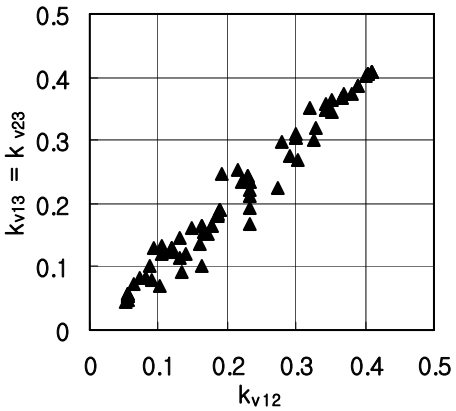

(b) k_{v12} vs k_{v13}

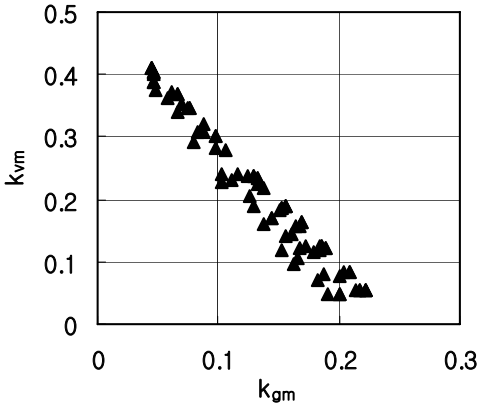

(c) k_{gm} vs k_{vm}

Fig.7 Relationships among elastic parameters.

(case 1. 2-layer body)

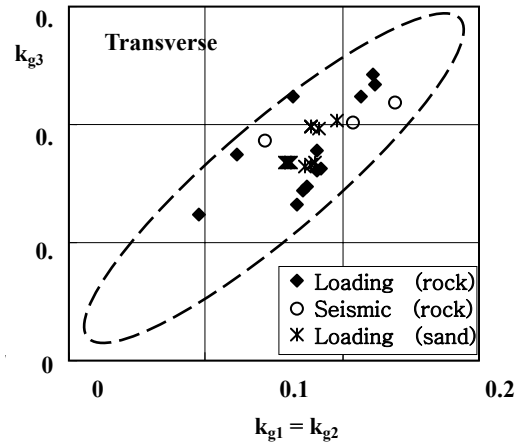

(a) k_{g1} vs k_{g3}

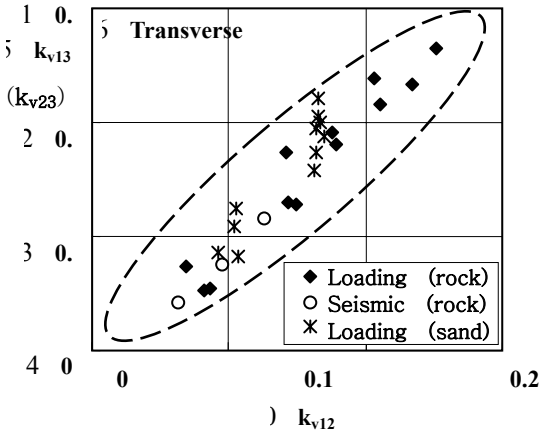

(b) k_{v12} vs k_{v13}

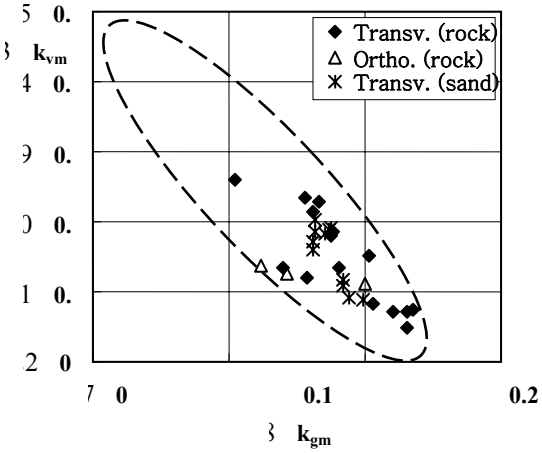

(c) k_{gm} vs k_{vm}

Fig.8 Relationships among elastic parameters.

(measured data for rock and sand, see Table 6)

5. Formulating back analysis to determine anisotropy

5.1 Premises about testing

The rock sample we are going to test for determining anisotropy is a hollow cylinder. A number of displacement censors are installed in the center hole. The both ends of the cylinder are capped, the entire cylinder is jacketed and the specimen is hydrostatically pressurized to a level roughly similar to the in-situ stress. The ratio between internal and external diameters of the cylinder is 1/4. The ratio is the restriction coming from the usage of the simple solution discussed in chapter 3 and especially in 3.2.1. The number of the displacement sensors need to be more than the number of unknown parameters of the anisotropy. When the directions of the anisotropic axes are unknown, there are in all 7 unknown parameters for the simplified orthogonal anisotropy, C_{11}, C_{22}, C_{33}, k_{gm}, θ_1, θ_2 and θ_3. Since a overcoring stress measurement technique used widely in Japan is usually adopting 8 displacement sensors, we are going to discuss whether 8 sensors are enough or not to stably determine the anisotropy through back analysis. If 8 sensors are good enough, then we will be able to use the same testing method and devices for the anisotropy determination. The directions of the 8 sensors are conceptually shown in Fig.9, namely, 4 horizontal directions and other 4 in inclined directions. Both ends of each sensor touch the wall of center hole via mortar.

Table 6. References for measured anisotropy data for rock and sand, plotted in Fig.8.

reference	rock	
(13)	Dolomite	TR
(13)	Dolomitic limestone	TR
(13)	Limestone	TR
(13)	Shaly limestone TR	
(13)	Fossiliferous limestone	TR
(13)	Limestone	TR
(13)	Black shale	TR
(13)	Shale	TR
(8)	Loveland sandstone I	TR
(8)	Loveland sandstone I	TR
(8)	Loveland sandstone II	TR
(8)	Loveland sandstone II	TR
(8)	Loveland sandstone II	TR
(8)	Loveland sandstone I	TR
(1)	Andesite (Sanjome)	TR
(1)	Granite (fine grained)	TR
(14)	Tuff (Ogino)	TR
(14)	Granite (Oshima) OR	
(15)	Shale (Queenstone)	TR
(16)	Slate	OR
	sand	
(18)	Ticino sand	TR
(*)	Kenia sand	TR

TR : transeversely anisotropy

OR : orthotropic anisotropy

(*) : personal letter

Table 7. Elasticity matrix for orthogonal anisotropy with reduced number of independent parameters.

C_{11}	$k_v(C_{11}+C_{22})$	$k_v(C_{11}+C_{33})$	0	0	0
	C_{22}	$k_v(C_{22}+C_{33})$	0	0	0
		C_{33}	0	0	0
			$k_g(C_{22}+C_{33})$	0	0
	Sym.			$k_g(C_{33}+C_{11})$	0
	(Note : k_v=1/2-2k_g*)*				$k_g(C_{11}+C_{22})$

5.2 Back analysis procedure

The simple solution eq.(1) is for the pressurization only on the outer lateral surface and not on the both ends. In the actual testing mentioned above, axial loading 16/15 times that on the lateral surface is added. 16/15 is the correction of cross section area of the center hole. Since the elastic response to the axial loading can be simply calculated, it is added to the simple solution u_r^{H}, u_z^{H} and ε_z^{H} to obtain the center hole deformation corresponding to the testing condition, as follows.

$$U_r^{H} = u_r^{H} + u_r^{ax}$$
$$U_z^{H} = u_z^{H} + u_z^{ax}$$
$$E_z^{H} = \varepsilon_z^{H} + \varepsilon_z^{ax} \qquad (8)$$

Here, u_r^{ax}, u_z^{ax} and ε_z^{ax} are the displacements in directions r and z and strain in z by the axial loading 16/15 times the pressurization.

Eq.(8) is the solution of deformation of center hole for the loading condition of actual testing, and thus enables the forward analysis to calculate U_r^{H}, U_z^{H} and E_z^{H}. The displacements measured by the 8 sensors in the center hole can be easily obtained using eqs.(8). As a result, we can forwardly calculate the displacement U_i of i^{th} sensor using the 7 parameters for the simplified orthogonal anisotropy even if we do not know the directions of the anisotropic axes.

$$U_i = f_i(C_{11}, C_{22}, C_{33}, k_g, \theta_1, \theta_2, \theta_3) \qquad (9)$$

Since we are going to use 8 sensors, we may be able to determine the 7 unknown parameters C_{11}, C_{22}, C_{33}, k_g, θ_1, θ_2 and θ_3 using the 8 measurements, through back analysis based on iterative convergence technique similar to nonlinear least squares regression.

The definition of θ_1, θ_2 and θ_3 are set in this paper as shown in Fig.10. θ_1 is the dip of major anisotropic plane on the X-Y surface. θ_2 is the dip direction measured from –Y toward –X. θ_3 is the rotation around the normal of the major anisotropic plane. The order of the three rotations is first (a), then (b) and finally (c) in Fig.10. Before the rotation (a), the anisotropic axes and coordinate X-Y-Z are agreeing with each other.

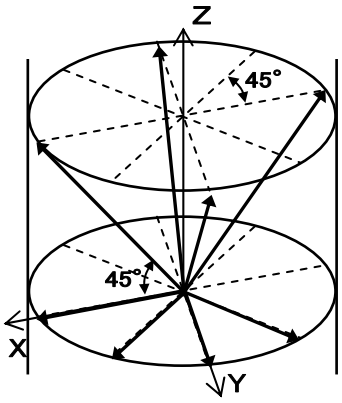

Fig.9 Directions of 8 displacement sensors in the center hole.

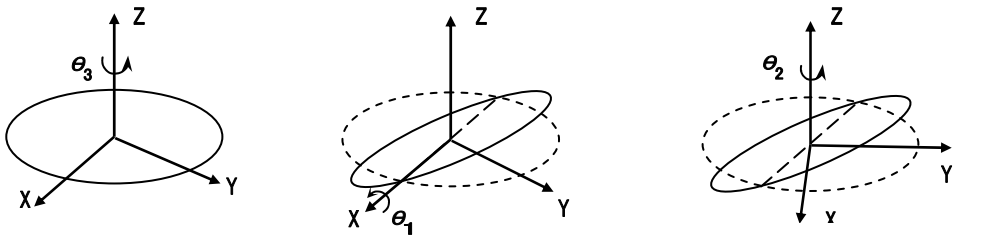

(a) θ_3 rotation around Z (b) θ_1 rotation around (c) θ_2 rotation around Z

Fig.10 Procedure of rotations.
In the order (a), (b) and (c).

5.3 Confirmation of stability of back analysis

Generally speaking, back analysis does not always give a unique answer but can give some false answers when the converging path falls into a local pit-hole. Therefore the objective of this section is to make clear whether the present back analysis described so far is stable or not.

The anisotropy set for this purpose is shown in Table 8. The ratio of anisotropy of normal elasticity, C_{11}/C_{33} is 2, and rotation transformation is applied 3 times. The specimen of hollow cylinder is supposed to be taken out in z direction from such orthogonal anisotropic rock. Then corresponding to the test procedure described in section 5.1, the normalized displacements in 8 directions are calculated using eqs.(9). These 8 values are the input for the back analysis to determine the anisotropy and its direction.

Table 8. Anisotropic parameters to be used for back analysis.

C_{11}	20		θ_1	30	
C_{22}	17		θ_2	30	
C_{33}	10		θ_3	30	
k_g	0.15				
7.416	7.013	5.871	-0.646	-0.558	-1.025
7.0125	17.646	5.917	-1.616	-0.223	-1.025
5.871	5.917	11.938	-1.616	-0.558	-0.41
-0.646	-1.616	-1.616	4.438	-0.308	-0.167
-0.558	-0.223	-0.558	-0.308	4.403	-0.485
-1.025	-1.025	-0.41	-0.167	-0.485	5.259

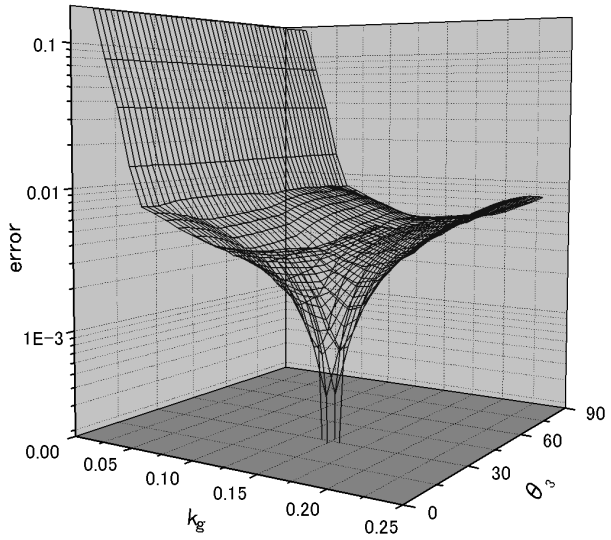

Fig.11 An example of convergence characteristics of back analysis.

(Distribution of residual error on k_g-θ_3 plane)

To observe the performance of convergence visually, the following study has been done. The variables k_g and θ_3 are fixed to every combination and other 5 unknown variables have been determined by the back analysis of present scheme. Then the residual errors are drawn on the k_g-θ_3 plane. The resultant 3D bird's eye view is shown in Fig.11. From the figure, we can see that the residual error is zero when k_g and θ_3 are correct, and thus correct answer is being derived. Also we can see that there are no local pit hole that can hinder to obtain the correct answer in the converging path. This means that even if we do not know the correct values of k_g and θ_3, we can come to the correct answer by the back analysis.

The above-mentioned verification of the stability of the back analysis is for the anisotropy case shown in Table 8, and we cannot deny that some special cases exist for which we may get into some pit holes. But basically the stability of the present method has been manifested.

Rocks and soil grounds often have visible anisotropic plane such as bedding. In such cases, 2 of the 3 parameters about the direction of the anisotropy are known. Then the resultant number of unknown parameters is 5 and the stability of back analysis will much improve.

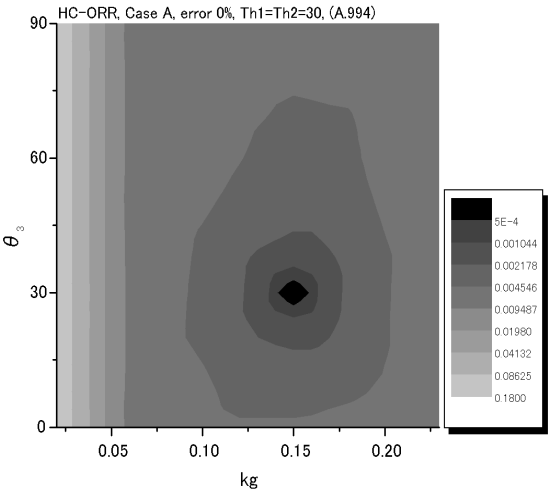

(a) 0% input error.

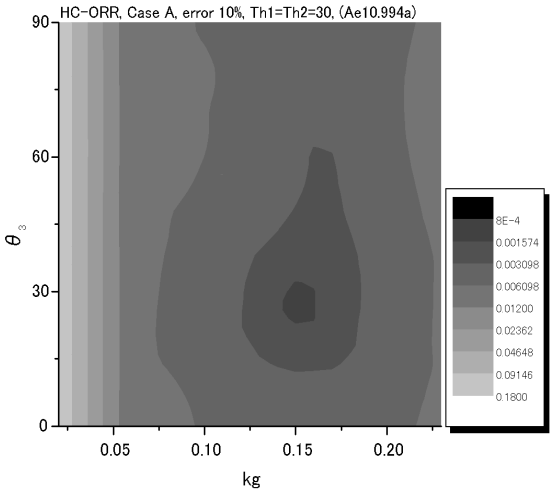

(b) an example for 10% input

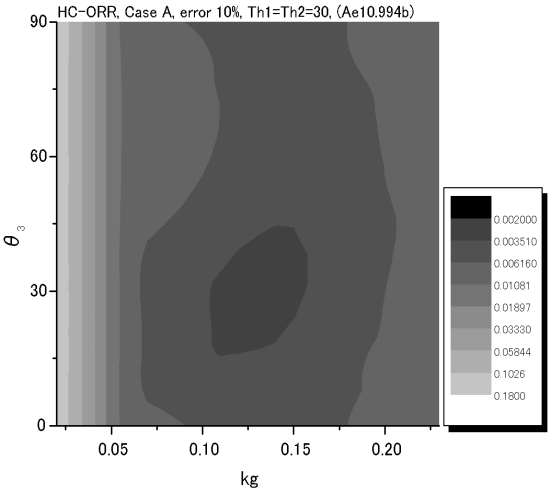

(c) an example for 10% input

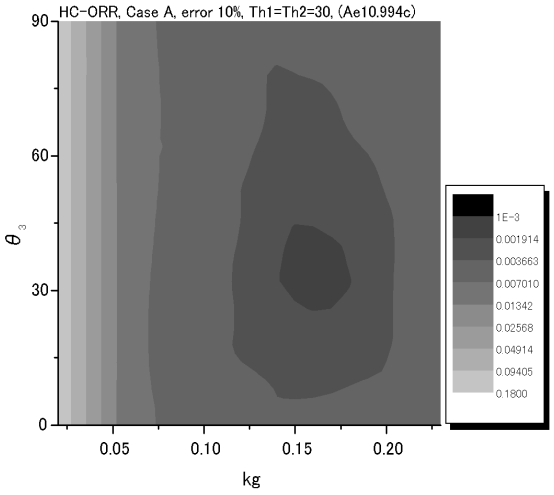

(d) an example for 10% input

Fig.12 Convergence characteristics for cases with no input error (a), and 10% input error (b), (c) and (d) (Distribution of residual error on k_g-θ_3 plane)

5.4 Influence of measurement error on the stability

In the previous section 5.3, the deformation in the center hole used as the input to the back analysis has been the exact value of theoretically calculated deformation by eqs.(9). But actual measurement of the deformation cannot be free from some error. Moreover, even if there is no measurement error in the center hole deformation, true anisotropy can be different from the simplified orthogonal anisotropy presented as Table 7 in chapter 4. Therefore, it has been of interest to clarify the influence of the error on the stability of back analysis. For this purpose, some errors have been added to the exact value of deformation and used as input to the back analysis.

Fig.12 is similar to Fig.11 but drawn 2 dimensionally. The residual error is not on the 3rd axis but shown as shading on k_g-θ_3 plane. Fig.12(a) is just for the case in Fig.11 with no measurement error. Fig.12(b), Fig.12(c) and Fig.12(d) are the results of 3 examples of the case with 10% error in the input value to the back analysis. 10% error has been generated as uniform random value with 10% width of the exact value of theoretical deformation. In the three cases, back analyzed values of k_g and θ_3 may be

a little different from the exact values of 0.15 and 30 degrees. The differences are within 0.025 for k_g and 5 degrees for θ_3. The shading patterns in the figures (b), (c) and (d) reveal that the back analysis is stable even if the input value contains errors in the order of 10%.

5.5 Conclusion about the back analysis

It has been verified that measurement of deformation in the center hole of a cylinder enables us to determine the orthogonal anisotropy of the specimen even when we do not know the directions of the anisotropic axes. It has also been demonstrated that the back analysis necessary for the determination is stable and does not lead to false results even when about 10% measurement error exists.

6. Conclusion

In the conventional geo-engineering for important infrastructure, plate jack test has been conducted to determine deformability of the rock. For future's necessity to determine its anisotropy for more rational design and for more detailed evaluation of rock behaviour, a method of determining anisotropy has been developed adopting the similar testing size as the plate jack test. The method has the following features.

The method is based not on a seismic test but on a loading test. Anisotropy at the in-situ static load level is determined by a pressurization test of a hollow cylinder.

Since the load is applied by pressurization, there is no fear of eccentric loading and the test is easy to perform.

The size of the specimen is large, in the order of a few tens centimeter to a meter. So the damage in the rock caused by sampling can be expected to be small.

The method theoretically requires only one specimen to determine a set of anisotropy. So the method is efficient and is not likely to be disturbed by variability of properties.

The method can determine orthogonal anisotropy and it is true even when the directions of the anisotropy are unknown.

This paper has noted the outline of the development of the method and demonstrated that the method is robust and practical through some simulations. In the future, a measurement device adequate for the method wants to be developed and the method wants to be applied to practical engineering.

References

1) Shin, K. and T. Kanagawa: Development of new method for elastic wave measurement and some experimental study on rock anisotropy., CREIPI report U90022, 1990. (in Japanese)
2) Chubu Electric Power Co.: Hamaoka Genshiryoku Hatsudensho Genshiro Setti Henko Kyoka Shinseisho (5 Go Ro Zosetsu)., 1997. (in Japanese)
3) Pinto, J.L.: The transversely isotropic body and its application to the study of the deformability of the schistous rocks., A research officer thesis, Laboratorio Nacional de Engenharia Civil, Lisboa Portugal, 1969.
4) Vinik, L.P., L.I. Makeyeva, A. Milev and A.Yu Usenko: Global Patterns of Azimuthal Anisotropy and Deformations in the Continental Mantle., Geophys J Int, Vol.111, No.3, pp.433-447, 1992.
5) Nakamura, M., M. Ando, K. Kusunose and T. Sato: Depth-dependent crustal anisotropy at Midwestern Honshu, Japan., Geophys Res Lett, Vol.23, No.23, pp.3417-3420, 1996.
6) Amadei, B.: Rock anisotropy and the theory of stress measurements., Lecture Notes in Engineering, Edited by C A Brebbia and S A Orszag 2, Springer-Verlag, 1983.
7) Ohkami, T., Y. Ichikawa and T. Kawamoto: A boundary element method for identifying orthotropic material parameters., Int J Numer Anal Methods Geomech, Vol.15, No.9, pp.609-625, 1991.
8) Amadei, B.: Importance of anisotropy when estimating and measuring in situ stresses in rock., Int J Rock Mech Min Sci & Geomech Abstr. 33(3), 293-325, 1996.

9) Sano O., K. Ishida, T. Hirano and Y. Kudo: A method for determination of elastic moduli of anisotropic rockmass with sound velocities of dilatational waves., Proc JSCE 589/III-42, 21-30, 1998. (in Japanese)
10) Oka, C. and K. Hirashima: Jack Shiken oyobi Suishitsu Shiken niyoru Ihosei Ganban Bussei no Kettei Hoho ni Kansuru Kenkyu., No.469/III-23, 83-91, 1993.
11) Hudson, J.A.: Wave speeds and attenuation of elastic waves in material containing cracks., Geophys J R astr Soc. 64, 133-150, 1981.
12) Salamon, M.D.G.: Elastic moduli of a stratified rock mass., Int J Rock Mech Min Sci & Geomech Abstr. 5, 519-527, 1968.
13) Lo, K.Y. and M. Hori: Deformation and strength properties of some rocks in southern Ontario, Can. Geotech. J. 16, 108-120, 1979.
14) Kawashima, S., O. Sano, Y. Mizuta and S. Ogino: Ihosei Ganseki no Danseiritsu Kettei ni tsuite., Spring Conf. 2101, 1987.
15) Hefny, A.M. and K.Y. Lo: Analytical solutions for stresses and displacements around tunnels driven in cross-anisotropic rocks., Int J Numer Anal Methods Geomech, 23, 161-177, 1999.
16) Homand,F., E. Morel, J.-P. Heyry, P. Cuxac and E. Hammade: Characterization of the moduli of elasticity of an anisotropic rock using dynamic and static methods., Int J Rock Mech Min Sci & Geomech Abstr. 30(5), 527-535, 1993.
17) Aleksandrov, K.S. and G.T. Prodayvoda: The study of elastic symmetry and anisotropy of elastic body waves in gneiss., Geophys. J. Int. 119, 715-728, 1994.
18) Bellotti, R., M. Jamiolkowski, D.C.F.Lo Presti and D.A. O'Neill: Anisotropy of small strain stiffness in Ticino sand., Geotechnique, Vol.46, No.1, p.115-131, 1996.